Integrated 3D inversion of magnetotelluric and HeliTEM data collected in the geothermal area of Japan

Alexander Gribenko, Leif Cox, Michael Jorgensen, and Michael S. Zhdanov, Consortium for Electromagnetic Modeling and Inversion, University of Utah, and TechnoImaging*
Masami Ikeya and Yusuke Usui, Exploration and Production Department, Idemitsu Kosan Co., Ltd.

Summary

Geothermal energy has become an attractive renewable source of energy around the globe. Developing effective geophysical methods for geothermal exploration is vital for studying these resources. It is well known that electric conductivity is an important indicator of the location of geothermal sources. One of the most widely used geophysical techniques for analyzing the deep electrical conductivity structure is the magnetotelluric (MT) method. At the same time, the airborne electromagnetic (EM) surveys represent effective methods for the near-surface conductivity study. In this paper, we jointly analyze the Helicopter Transient Electromagnetic (HeliTEM) and magnetotelluric (MT) data acquired in some geothermal areas of Japan. The advantage of this approach over the analysis of the MT data alone is related to the fact that MT data are strongly affected by the near-surface inhomogeneities. Furthermore, the airborne HeliTEM data provide complementary information about the near-surface conductivity distribution, which we use to constrain the results of MT inversion. Thus, the joint interpretation of MT and HeliTEM data produces more reliable information about the deep conductivity model. This paper discusses the methods of 3D inversion of HeliTEM data and how to use these data in 3D MT inversion. The developed approach to the joint interpretation of the HeliTEM and MT data is illustrated by practical inversion of the HeliTEM and MT data collected over the geothermal field in Japan.

Introduction

Japan Oil, Gas and Metals National Corporation (JOGMEC) commissioned Helicopter Transient Electromagnetic (HeliTEM) data acquisition in the geothermal prospect area of Japan. Approximately 1366 line-km of HeliTEM data at 250 m line spacing in an east-west direction were collected by CGG on behalf of JOGMEC in 2017. Figure 1 shows the fight lines of the survey located within the area of interest (AOI).

At the same time, Idemitsu Kosan Co., Ltd.(Idemitsu) also collected a total of 160 stations of MT data in the same AOI (Figure 1). Part of MT data was obtained with the support of the JOGMEC grant.

There are many publications related to applying the magnetotelluric (MT) method to study geothermal systems (e.g., Wannamaker et al. 2004; Newman et al. 2008). However, until recently, airborne EM data were rarely used for this purpose. This paper demonstrates that the joint interpretation of the airborne EM and MT data increases the effectiveness of geoelectrical studying the geothermal fields.

We have developed an efficient method of full rigorous 3D inversion of HeliTEM data. This method was applied to the HeliTEM data collected over the selected AOI.

We have processed and inverted in 3D all the MT data shown in Figure 1. In the final data analysis stage, we have conducted an integrated interpretation of magnetotelluric and HeliTEM data collected over an area of interest (AOI) in Japan (Figure 1). The goal is to construct a 3D model of the subsurface resistivity distribution to satisfy both the observed HeliTEM and MT data. Due to the MT station spacing and plane-wave structure of the source, MT data have less resolution to the shallow conductivity distribution. Therefore, inaccuracies in near-surface conductivity may result in the erroneous determination of deeper conductivity structures.

On the other hand, HeliTEM data have superior sensitivity to the conductivity distribution to the depths up to 500 m. The HeliTEM inverse model provides essential information about the near-surface conductivity distribution in the survey area. In the joint HeliTEM – MT inversion, it is used to constrain the near-surface geoelectrical structure, also affecting the deep anomalies produced by MT inversion.

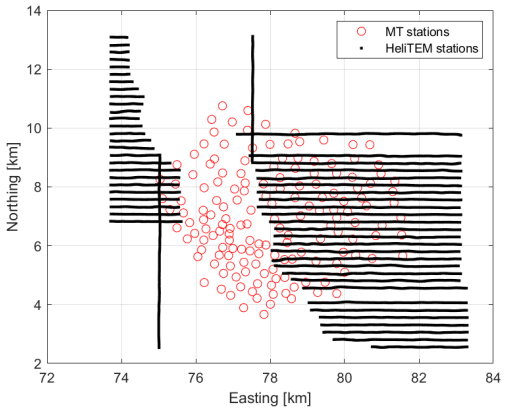

3D inversion of HeliTEM data

The goal of inversion is to recover the 3D conductivity distribution from the HeliTEM data. However, HeliTEM survey data are contaminated with noise, and the inverse

model may change dramatically while keeping the predicted data within the noise level. This means that the inversion is ill-posed; i.e., solutions are nonunique and unstable (Zhdanov, 2002, 2015, 2018). One has to use regularization to obtain a unique and stable solution. This can be achieved by minimization of the Tikhonov parametric functional, $P^{\alpha}(\boldsymbol{\sigma})$:

$$P^{\alpha}(\boldsymbol{\sigma}) = \|\boldsymbol{W}_d(\boldsymbol{A}(\boldsymbol{\sigma}) - \boldsymbol{d}_{obs}\|^2 + \alpha\left\|\boldsymbol{W}_{\boldsymbol{m}}(\boldsymbol{\sigma} - \boldsymbol{\sigma}_{apr})\right\|^2 \rightarrow min, \quad (1)$$

where $\boldsymbol{A}$ is the nonlinear forward modeling operator, $\boldsymbol{\sigma}$ is the vector of conductivities, $\boldsymbol{d_{obs}}$ is the vector of observed data, $\boldsymbol{\sigma_{apr}}$ is the of the a priori conductivities, and ‖... ‖denotes the respective least-square norm.

We use both one-dimensional (1D) and three-dimensional (3D) inversions to process the data. In our standard workflow, 1D inversion is used to QC the data and create an approximate background model, while 3D inversion is used for final, higher accuracy inversion runs. One-dimensional inversion is typically faster than 3D inversion and can produce accurate models in areas where the earth is laterally invariant. The 1D approximation is used to speed up calculations and assumes that the earth is layered, and these layers extend to infinity horizontally. Each transmitter-receiver position, or sounding location, has a 1D layered earth model under it, which is recovered during inversion. These are then gridded into a 3D model to create a more realistic earth picture, but the modeling and physics are inaccurate. Only the Z (vertical) component can be used because a 1D earth does not create an appreciable electromagnetic field in the X or Y direction with a small offset system like HeliTEM. Hence, with 1D inversion, almost half the data are ignored, and this is the data that responds best to lateral variations in conductivity and produces high-resolution images.

In contrast, 3D inversion considers all the geometry of the targets of the earth and can use both horizontal and vertical components of the data. The recovered models are thus much more accurate, especially in areas with complex geometry and geology, but this is at the expense of much more complex algorithms and a large volume of computations. We have developed an effective method and advanced software package EMVision® capable of large-scale 3D inversions (see Cox and Zhdanov, 2007, and Zhdanov, 2018, for details).

All inversions were carried out using the developed EMVision® software package. The software uses a robust and stable method to solve for the 3D physical parameter distribution in the earth. Fast and accurate algorithms based on the integral equation method are used to model physics properly. Flexibility in the software allows a wide selection of stabilizers, a priori models, and cooperative inversion techniques (Zhdanov, 2015). The inversion method uses data weights to ensure fitting of the data to the appropriate noise level and model weights to normalize sensitivities of the data for increased depth resolution and stability.

HeliTEM inversion results

The developed method of 3D inversion was applied to the HeliTEM data collected over the AOI shown in Figure 1. The helicopter was maintained at a mean altitude of 128 meters above the ground during the survey. The transmitter coil was located 47 m below the helicopter. The transmitter was a single loop with an area of 708 m^2 and a peak current of 1538 A. The source waveform was a half-sine. The receiver loop was 26.7 above and 12.9 m forward of the transmitter loop center. The receiver measures three dB/dt field components in the horizontal (X along line and Y cross-line) and vertical (Z) directions. The base frequency of the system was 25 Hz. Four on-time channels and 26 off-time channels from 88 μs to 14.2 ms (midpoint) were measured. We have performed 3D inversion of HeliTEM data using all available offtime channels.

The final workflow for the inversion was to run the 1D inversion using EMVision® on the Z component data. This initial inversion step uses 1D sensitivities but full 3D stabilizers and runs on a voxel discretization of the model exactly like the 3D inversion. The model for the 1D inversion was discretized into 50 m x 50 m cells in the inline and cross-line directions horizontally. The vertical discretization was 18 cells from 5 m thick at the surface to 50 m thick at depth. The total thickness of the inversion domain was 640 m. These 1D inversions were used for initial quality control of the model. The stitched-together results of 1D inversions were smoothed by a 3 x 3 x 1 (x by y by z) cell size boxcar function. The resulting 3D model was used as a variable background conductivity model for the full rigorous 3D inversion.

The 3D inversion used a minimum norm stabilizer combined with a 2nd derivative in the crossline and vertical directions. The stabilizer ensures the algorithm finds a geologically reasonable model which also satisfies the observed data. A 1e-4 S/m (10,000 Ohm-m) hard lower bound was used in the inversion. No upper bound was needed.

After analysis of the background 1D result and further testing, it was determined that the optimal horizontal cell sizes for the full 3D inversion were 25 m x 50 m in the inline and cross-line directions, and the same vertical discretization was used as for the 1D model. The convergence of the inversion using these errors as data weights is given in Figure 2. One can see that RMS reached 2.5 after about 500 iterations.

Figure 3 shows an example of observed and predicted data along line 60290. The Z component fits well, but the X and Y channels were noisier and were not fit as tightly on purpose so as not to fit noise in the data. Much of this noise is likely due to bird swings. Also, the geology in the study

area did not exhibit strong lateral contrasts, so these responses were subdued.

Figure 4 shows an example of the vertical cross section of the 3D resistivity distribution recovered from unconstrained inversion of HeliTEM data along a profile.

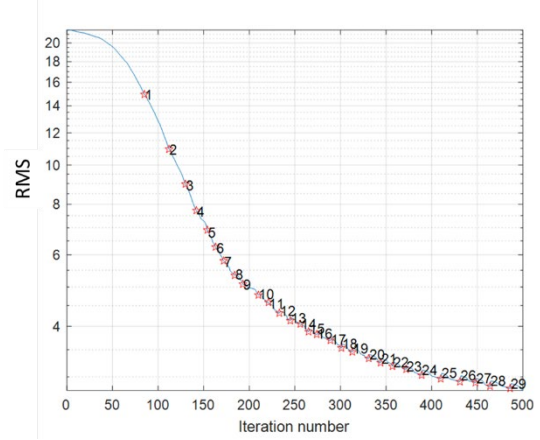

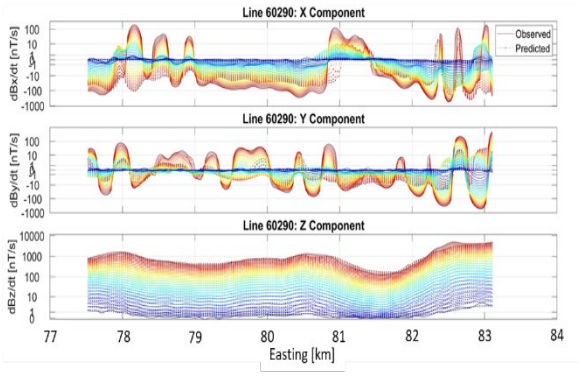

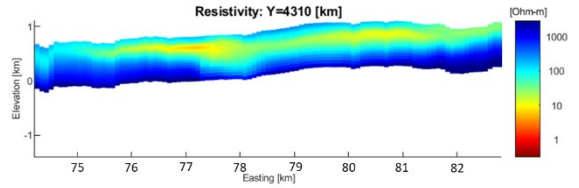

3D inversion of MT data

The magnetotelluric inverse problem can be formulated as the solution of the following operator equation:

$$\mathbf{d} = \mathbf{cZ} \quad = \mathbf{cA}(\boldsymbol{\sigma}), \tag{2}$$

where $\mathbf{A}$ is the forward modeling operator based on MT transforms and the IE method, $\mathbf{Z}$ is the impedance tensor, and $\mathbf{c}$ is a distortion matrix, which considers the effects of geoelectrical inhomogeneities in the locations of the MT stations. The inversion is run simultaneously for the components of the distortion matrix, $\mathbf{c}$, and 3D conductivity distribution, $\boldsymbol{\sigma}$ (Gribenko and Zhdanov, 2017).

We apply the standard Tikhonov regularization approach (Zhdanov, 2015) to find conductivity distribution that fits the observed impedance data to an acceptable misfit level. Within the Tikhonov regularization framework, we minimize parametric functional $P(\boldsymbol{\sigma}, \mathbf{c})$ containing two terms – data misfit $\|\boldsymbol{r}\|^2$ and stabilizer $\|\mathbf{S}\|^2$ (model misfit) with regularization parameter α used to balance the input of the two terms:

$$\begin{aligned} P(\boldsymbol{\sigma}, \mathbf{c}) &= \|\mathbf{r}\|^2 + \alpha\|\mathbf{S}\|^2, \\ \mathbf{r} &= \mathbf{W}_d(\mathbf{cA}(\sigma) - \mathbf{d}\text{obs}), \\ \mathbf{S} = \mathbf{W}_m \begin{bmatrix} \mathbf{S}_\sigma \\ \mathbf{S}_\mathbf{c} \end{bmatrix} &= \mathbf{W}_m \begin{bmatrix} \mathbf{L}(\boldsymbol{\sigma} - \boldsymbol{\sigma}_\mathrm{b}) \\ \mathbf{c} - \mathbf{c}_0 \end{bmatrix} \\ \mathbf{W}_m &= diag(\mathbf{F}^T\mathbf{F})^{0.25}. \end{aligned} \tag{3}$$

In the above equations $\mathbf{W}_d$ represents data weights based on the inverse of variances or the data noise floor, $\boldsymbol{\sigma}_\mathrm{b}$ is the background conductivity model, $\mathbf{c}_0$ - zero distortion (identity) matrix, $\mathbf{L}$ – first-order finite difference matrix, and $\mathbf{F}$– the Fréchet derivative (sensitivity) matrix.

Note that for the constrained inversion background conductivity model $\boldsymbol{\sigma}_\mathrm{b}$ is replaced by the a priori model $\boldsymbol{\sigma}_\mathrm{apr}$. The same model is also used as an initial for the inversion.

We use the Newton method in data space to minimize parametric functional. Newton's method ensures fast convergence and optimal computer memory management.

Results of standalone MT inversion

We have analyzed the observed MT data consisting of four components of the full MT tensor. We have selected the frequency range: 0.01 – 100 Hz (acceptable noise level and coverage of the AOI).

We have performed unconstrained standalone 3D inversion of MT data without any constraints. The RMS misfit converges to 1.39. Figure 5, Panel A, shows the vertical section of the 3D resistivity distribution recovered from inversion of MT data, along with the same profile I (left panel) as shown in Figure 4 for HeliTEM data inversion.

Geoelectrical model produced by the integrated inversion of the HeliTEM and MT data

It is well known that the near-surface geoelectrical inhomogeneities could significantly affect the results of MT

data inversion at the depth. However, this effect can be substantially reduced if the near-surface geoelectrical model is known and used as a constraint for MT inversion. Following this concept, we have performed constrained 3D inversion of MT data using HeliTEM inversion results as constraints.

Note that the HeliTEM inverse model only extends to 600 m depth from the earth's surface. At a greater depth, and where HeliTEM data coverage was insufficient, this model was complemented by the result of 1D MT inversion. The RMS misfit converges to 1.34. Figures 5, Panel B, presents the vertical cross sections of the 3D resistivity distribution recovered by joint inversion of HeliTEM and MT data.

One can see from Figure 5 that the geoelectrical model recovered from the constrained inversion clearly indicates the presence of a highly conductive zone in the north-eastern part of the survey area, which extends at a depth of about one km. The resolution of the shallow structures is also improved, and the artifacts in the deeper layers disappear in the case of joint inversion.

Figure 6 compares the resistivity model obtained from joint inversion of HeliTEM and MT data with the schematic geological section based on the surface geology and a few wells, along with the same profile. Again, we can see a good qualitative correlation between the geoelectrical model and the schematically reconstructed geology of the area.

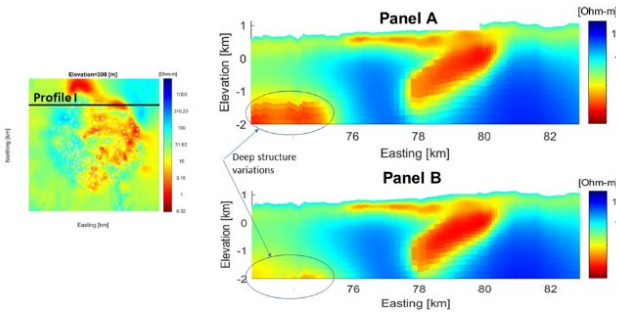

Figure 5: Vertical sections over Profile I of the inverse resistivity models produced by standalone MT inversion (Panel A) and joint inversion of HeliTEM and MT data (Panel B).

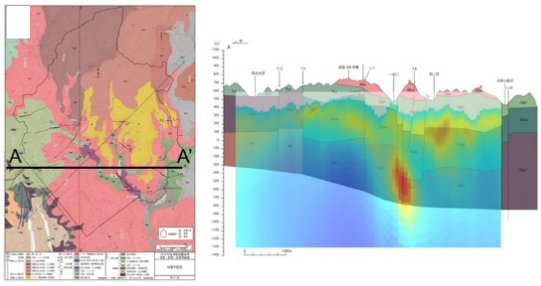

Figure 6: The resistivity model is superimposed on the geologic section (right panel) over profile AA', shown in the left panel.

Conclusions

The results of integrated inversion of airborne HeliTEM and MT data collected over known geothermal field in Japan have demonstrated the practical effectiveness of this approach. Both deep and shallow conductive features have been resolved, corresponding to the geothermal source and the reservoir. In addition, inversion added resolution to the near-surface conductive structures by using information about the near-surface resistivity distribution obtained from the HeliTEM data. This also improves the accuracy of MT inversion for the main conductive anomaly compared to the standalone MT inversion.

Acknowledgments

The authors acknowledge TechnoImaging, the Consortium for Electromagnetic Modeling and Inversion (CEMI) of The University of Utah, Idemitsu Kosan Co., Ltd. and Japan Oil, Gas and Metals National Corporation (JOGMEC) for the support of this project and permission to publish.

REFERENCES

Cox, L. H., and M. S. Zhdanov, 2007, Large-scale 3D inversion of HEM data using a moving footprint: 77th Annual International Meeting, SEG, Expanded Abstracts, 467–471, doi: https://doi.org/10.1190/1.2792464

Gribenko, A. V., and M. S. Zhdanov, 2017, 3-D inversion of the MT EarthScope data, collected over the east central United States: Geophysical Research Letters, **44**, 11,800–11,807, doi: https://doi.org/10.1002/2017GL075000.

Newman, G. A., E. Gasperikova, G. M. Hoversten, and P. E. Wannamaker, 2008, Three-dimensional magnetotelluric characterization of the Coso geothermal field: Geothermics, **37**, 369–399, doi: https://doi.org/10.1016/j.geothermics.2008.02.006.

Wannamaker, P. E., P. E. Rose, W. M. Doerner, B. C. Berard, J. McCulloch, and K. Nurse, 2004, Magnetotelluric surveying and monitoring at the Coso geothermal area, California, in support of the enhanced geothermal systems concept: survey parameters and initial results: Presented at the Proceedings, 29th Workshop on Geothermal Reservoir Engineering, Stanford University.

Zhdanov, M. S., 2002, Geophysical inverse theory and regularization problems: Elsevier.

Zhdanov, M. S., 2009, New advances in regularized inversion of gravity and electromagnetic data: Geophysical Prospecting, **57**, 463–478, doi: https://doi.org/10.1111/j.1365-2478.2008.00763.x.

Zhdanov, M. S., 2015, Inverse theory and applications in geophysics: Elsevier.

Zhdanov, M. S., 2018, Foundations of geophysical electromagnetic theory and methods: Elsevier.

Zhdanov, M. S., A. Green, A. Gribenko, and M. Čuma, 2010, Large-scale three-dimensional inversion of EarthScope MT data using the integral equation method: Physics of the Earth, **8**, 27–35.